Letter

ADVANCED PHOTONICS

Mode-locked 2.8-μm fluoride fiber laser: from soliton to breathing pulse

Zhipeng Qin,[a,b,c] Guoqiang Xie,[a,b,c,*] Hongan Gu,[a,b,c] Ting Hai,[a,b,c] Peng Yuan,[a,b,c] Jingui Ma,[a,b,c] and Liejia Qian[a,b,c]
[a]Shanghai Jiao Tong University, School of Physics and Astronomy, Shanghai, China
[b]Shanghai Jiao Tong University, Collaborative Innovation Center of Inertial Fusion Sciences and Applications, Shanghai, China
[c]Shanghai Jiao Tong University, Key Laboratory for Laser Plasmas, Ministry of Education, Shanghai, China

Abstract. The mode-locked fluoride fiber laser (MLFFL) is an exciting platform for directly generating ultrashort pulses in the mid-infrared (mid-IR). However, owing to difficulty in managing the dispersion in fluoride fiber lasers, MLFFLs are restricted to the soliton regime, hindering pulse-energy scaling. We overcame the problem of dispersion management by utilizing the huge normal dispersion generated near the absorption edge of an infrared-bandgap semiconductor and promoted MLFFL from soliton to breathing-pulse mode-locking. In the breathing-pulse regime, the accumulated nonlinear phase shift can be significantly reduced in the cavity, and the pulse-energy-limitation effect is mitigated. The breathing-pulse MLFFL directly produced a pulse energy of 9.3 nJ and pulse duration of 215 fs, with a record peak power of 43.3 kW at 2.8 μm. Our work paves the way for the pulse-energy and peak-power scaling of mid-IR fluoride fiber lasers, enabling a wide range of applications.

Keywords: ultrafast fiber laser; mid-infrared; breathing pulse; mode-locking; dispersion management.

Received Oct. 9, 2019; accepted for publication Dec. 17, 2019; published online Dec. 27, 2019.

[DOI: 10.1117/1.AP.1.6.065001]

Mid-infrared (mid-IR) ultrafast µlaser sources are becoming increasingly attractive for a variety of applications ranging from spectroscopy to medical surgery.[1–5] In recent years, the mode-locked fluoride fiber laser (MLFFL) has emerged as a simple and cost-effective way to generate mid-IR ultrafast laser, as a compact, high-efficiency platform that features excellent beam quality. Femtosecond soliton mode-locking has been realized from fluoride fiber lasers near a wavelength of 3 μm using the nonlinear polarization rotation (NPR) technique.[6–9] These soliton mode-locked lasers generally have a nanojoule-order pulse energy and peak power of the order of 10 kW. However, many mid-IR applications, such as supercontinuum generation and material modification, require a higher pulse energy and peak power,[10–12] which are challenging to achieve in MLFFLs.

As fluoride fibers exhibit anomalous group velocity dispersion (GVD) in the mid-IR range, MLFFLs generally work in a soliton mode-locking regime through a balance between nonlinearity and anomalous dispersion. In a soliton mode-locking regime, the accumulated excessive nonlinear phase will cause soliton break-up, limiting the pulse-energy scaling according to the soliton area theorem. One feasible strategy to overcome this limitation is to manage intracavity dispersion. In conventional silica fiber lasers, the sign and amount of GVD can be conveniently engineered by ion doping or by designing structures in silica fibers. Thus mode-locked silica fiber lasers can operate in a wide range of regimes, such as stretched-pulse mode-locking, dissipative soliton, and similariton.[13–16] These regimes intrinsically operate in the chirped-pulse mode in the cavity, resulting in less nonlinear phase accumulation and supporting a high pulse energy and peak power. Current state-of-the-art mode-locked silica-fiber lasers support a pulse energy of the order of microjoules and a peak power of the order of megawatts with the help of dispersion management.[17] However, unlike silica fiber, fluoride fiber engineering remains an open problem, and current techniques cannot support the GVD engineering of fluoride fibers. It is critical to solve the dispersion-management problem of MLFFLs for pulse-energy and peak-power scaling.

In MLFFLs, fluoride fibers several meters long generally have a large anomalous dispersion ($\sim -10^5$ fs^2) at an operation wavelength of 2.8 μm.[6–9] It is nearly impractical to compensate for such a large anomalous dispersion using general bulk materials with normal GVD. However, we find that semiconductor material possesses a huge normal GVD near the absorption

*Address all correspondence to Guoqiang Xie, E-mail: xiegq@sjtu.edu.cn; Liejia Qian, E-mail: qianlj19@sjtu.edu.cn

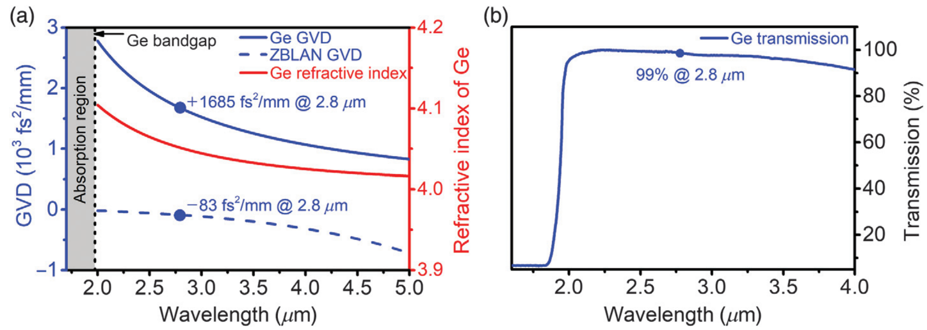

Fig. 1 (a) GVD and refractive-index curves of Ge and GVD curve of ZBLAN fiber. Sellmeier equations of Ge and ZBLAN are used from Refs. 18 and 19. (b) Transmission curve of 2-cm-long anti-reflection-coated Ge rod measured using a Fourier-transform spectrometer.

edge, which results from the rapid change of refractive index. For example, germanium (Ge) has an infrared bandgap (0.66 eV) and absorption region near 2 μm; in the near absorption edge of 2.8 μm, it has a huge GVD of $+1685$ fs^2/mm [Fig. 1(a)]. Such a GVD is more than 20 times that of fluoride fiber, which means that Ge rod a few centimeters in length is sufficient to manage the intracavity dispersion of MLFFLs. The combination of high transmission in the mid-IR range [Fig. 1(b)] and large positive GVD near the absorption edge makes such a semiconductor a reliable and practical method of dispersion management for MLFFLs.

In the present work, by utilizing the huge normal GVD generated near the absorption edge of Ge for dispersion management, we first realized breathing-pulse mode-locking in an Er-doped fluoride fiber laser. The pulse-energy-limitation effect was mitigated in the breathing-pulse mode-locking regime. The breathing-pulse MLFFL produced a pulse energy of 9.3 nJ and a pulse duration of 215 fs with a record peak power of 43.3 kW, which reaches the level of state-of-the-art mid-IR femtosecond optical parametric oscillators in the spectral region around 3 μm.[20,21] This work paves the way for the pulse-energy and peak-power scaling of mid-IR MLFFLs.

The mode-locked Er:ZBLAN fiber laser (Fig. 2) was pumped by a 970-nm laser diode pigtailed to a 105/125-μm fiber with a numerical aperture of 0.22. A set of lenses consisting of planoconvex lens L_1 ($f = 10$ mm) and aspheric lens L_2 ($f = 12.7$ mm) was used to couple the pump beam into the double-clad Er:ZBLAN fiber. The Er:ZBLAN gain fiber had a length of 2.3 m and 6 mol.% Er doping with a core diameter of 16.5 μm and cladding diameter of 200 μm. The two ends of the fiber were 8-deg angle-cleaved to suppress parasitic oscillation. Mode-locking operation was initiated and sustained through NPR using an isolator, a half-wave plate, and a quarter-wave plate. To reduce the mode-locking threshold in the experiment, we controlled the intracavity pulse propagation along the pump-light direction. An output coupler (OC) with 40% transmission was positioned after the gain fiber. Three Ge rods with different lengths ($L = 2$, 3, and 6 cm, corresponding to net cavity dispersions of -0.158, -0.141, and -0.090 ps^2, respectively) were prepared for dispersion management. The Ge rod introduces almost no insertion loss or nonlinear effect, which is beneficial to investigate the influence of dispersion on the dynamics of the mode-locked fiber laser. In particular, the huge GVD of Ge at the wavelength of

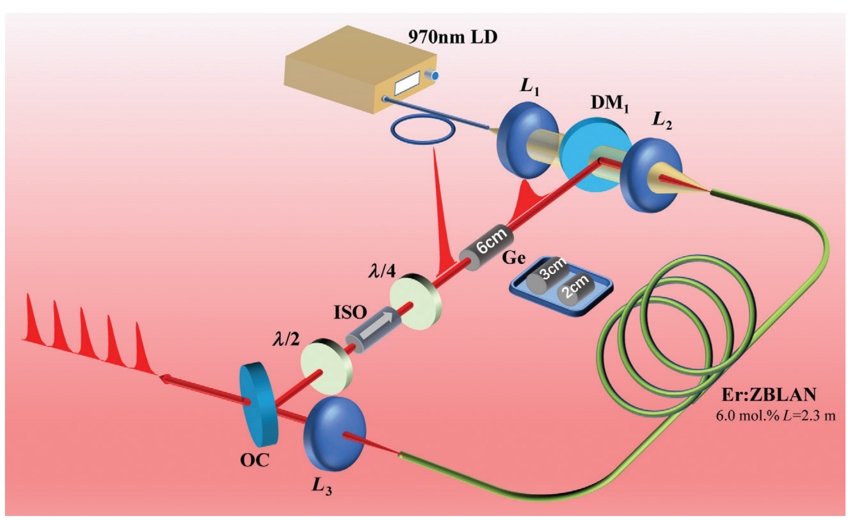

Fig. 2 Schematic of the breathing-pulse mode-locked Er:ZBLAN fiber laser. LD, laser diode; DM, dichroic mirror; OC, output coupler with a transmission of 40%; ISO, optical isolator; $\lambda/2$, half-wave plate; $\lambda/4$, quarter-wave plate; and Ge, germanium rod.

2.8 μm facilitates intracavity dispersion management using a short Ge rod.

Mode-locked operation was first conducted without dispersion management. Since fluoride fiber exhibits an anomalous GVD around 2.8 μm, the mode-locked laser operated in a soliton regime through a balance between nonlinearity and anomalous dispersion. Under a launched pump power of 7.7 W, stable continuous-wave mode-locking was achieved [Fig. 3(a)]. The radio-frequency spectrum shows a high signal-to-noise ratio of 70 dB at a fundamental frequency of 75.5 MHz [Fig. 3(b)]. The mode-locked pulse had a duration of 190 fs, assuming a sech^2 profile [Fig. 3(c)]. Despite the strong absorption by vapor in the atmosphere, Kelly sidebands can be identified in the spectrum [Fig. 3(d)], indicating soliton mode-locking. In the soliton regime, the mode-locked Er:ZBLAN fiber laser delivered a maximum pulse energy of 5.6 nJ. While further increasing the launched pump power in the experiment, the output pulse energy remained almost constant until multiple pulsing occurred [Fig. 4(d)].

In order to mitigate the limitation in pulse energy, we propose to manage the intracavity dispersion and promote the laser to the breathing-pulse mode-locking regime. An infrared-bandgap semiconductor with a huge normal GVD at 2.8 μm is utilized to compensate for part of the anomalous dispersion in the fluoride fiber laser. Since the net dispersion of the laser is negative, the output pulse is a transform-limited femtosecond pulse. After the OC, the pulse is first stretched in the semiconductor, then compressed in the front part of the fiber, and finally evolves into a soliton pulse near the exit of the fiber. Owing to the coexistence of normal and anomalous dispersion elements in the laser, the intracavity pulse is stretched and compressed successively in a round trip, acting as a breathing pulse. The breathing pulse effectively reduces nonlinear phase accumulation in the laser compared with soliton mode-locking. Thus higher pulse energy can be generated in a breathing-pulse mode-locked laser.

Guided by this breathing-pulse mode-locking concept, we conducted a mode-locking experiment of the Er:ZBLAN fiber laser. In the mode-locked laser, a Ge rod was used to compensate for partial intracavity dispersion, promoting the laser to the breathing-pulse regime. In the soliton regime without a Ge rod, the output pulse energy remains unchanged while increasing the pump power, as shown in Fig. 4(d). After dispersion compensation, the limitation effect of pulse energy is mitigated. At a fixed launched pump power of 7.7 W, the output pulse energy increases from 5.6 to 8.0 nJ with the increase of Ge rod length [Fig. 4(a)]. Meanwhile, the output pulse duration increases from 190 to 290 fs because the self-phase-modulation-induced spectral broadening effect becomes weak [Figs. 4(b)–4(c)]. In the breathing-pulse regime, since the pulse is stretched and compressed successively in the cavity, the accumulated nonlinear phase shift is significantly reduced compared with the soliton regime. The reduction of the accumulated nonlinear phase shift mitigates the pulse-energy-limitation effect. As we increase the launched pump power, the output pulse energy is further increased, as shown in Fig. 4(d). A maximum pulse energy of 9.3 nJ is achieved under a launched pump power of 11 W. As the intracavity pulse energy and peak power increase, the self-phase-modulation-induced spectral broadening effect becomes stronger, whereby the output pulse duration gradually decreases [Fig. 4(d)]. Eventually, 215-fs pulses with a pulse energy of 9.3 nJ are achieved directly from the breathing-pulse mode-locked Er:ZBLAN fiber laser [Fig. 4(e)], with a record peak power of 43.3 kW at 2.8 μm. Further increasing the peak power will pose a risk of damage to the end face of the fluoride fiber. A higher peak power might be achieved by splicing a protective end cap to the fluoride fiber.

Here, the employed Ge rod only compensates for a part of the anomalous dispersion of the entire fluoride fiber. The soliton-shaping effect still exists at the end of the fluoride fiber. According to the spectral width of 41.6 nm in the mode-locking

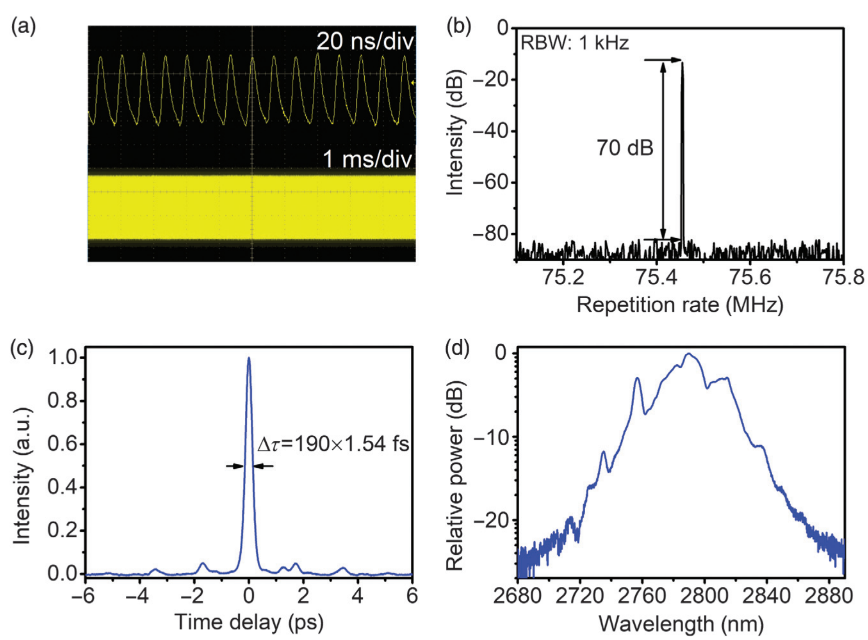

Fig. 3 Soliton mode-locked Er:ZBLAN fiber laser: (a) pulse trains in nanosecond and millisecond time scales, respectively; (b) radiofrequency spectrum; (c) measured intensity autocorrelation trace; and (d) mode-locked pulse spectrum.

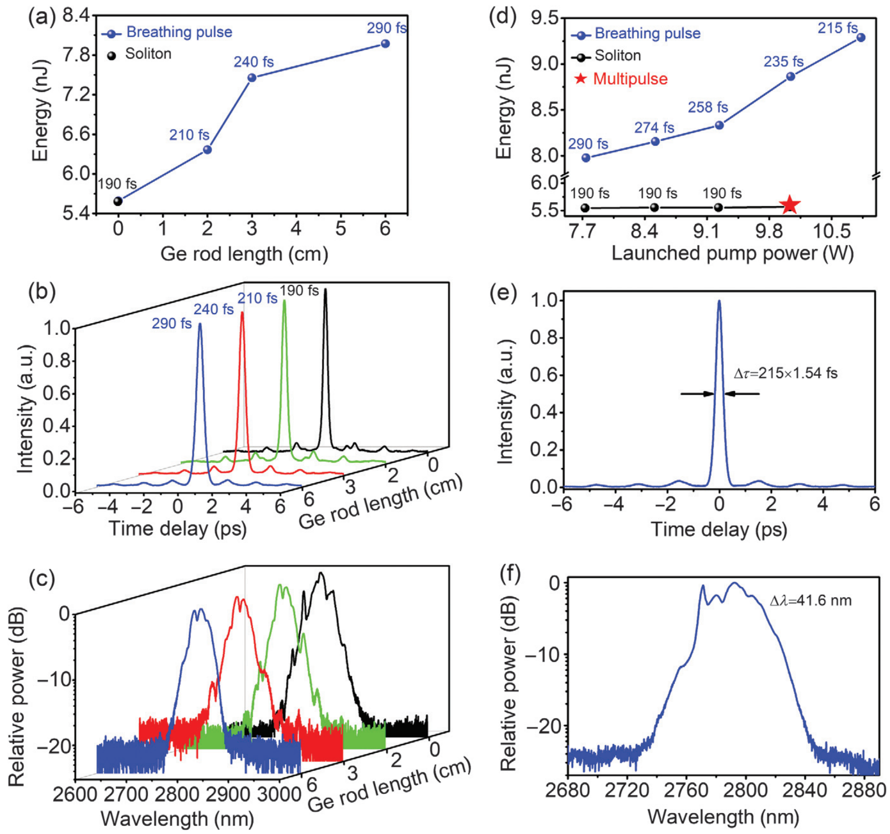

Fig. 4 Characteristics of the breathing-pulse mode-locked Er:ZBLAN fiber laser. Evolution of (a) pulse energy and duration, (b) autocorrelation trace, and (c) mode-locking spectrum with the Ge rod length. The net intracavity dispersions are −0.191, −0.158, −0.141, and −0.090 ps^2 for Ge rod lengths of 0, 2, 3, and 6 cm, respectively. Evolution of the (d) pulse energy and duration with the launched pump power in the soliton and breathing-pulse regimes. (e) Measured autocorrelation trace and (f) mode-locking spectrum for 9.3-nJ output pulses.

spectrum [Fig. 4(f)], we calculate the time-bandwidth product of the output pulses as 0.347, which is close to the transform-limited value. Intracavity net anomalous dispersion enables the generation of transform-limited pulses, avoiding extra pulse compression outside the cavity.

In order to confirm the pulse-breathing behavior along the cavity, the pulse evolution in the Er:ZBLAN fiber laser was investigated though numerical simulation in the time and frequency domains. The numerical simulation included the linear loss, dispersion map, Kerr nonlinear effect, saturable gain, and NPR action for reproducing the basic features of the experimental observations. The detailed simulation process can be found in Sec. 1 of the Supplementary Material. Figure 5 shows the evolutions of pulse duration, spectrum, and pulse energy with the position in cavity. When a near-transform-limited pulse passes through the Ge rod, it is stretched quickly by the normally dispersive Ge, resulting in a long pulse before amplification in the fluoride fiber. Because the low levels of loss and nonlinear effects in Ge can be neglected, the pulse energy and spectrum remain unchanged in the Ge rod. Consequently, the positively chirped pulse is amplified and compressed gradually in the anomalously dispersive fluoride gain fiber. At the end of the fluoride fiber, the compressed pulse evolves into a soliton through the balance of the anomalous dispersion and nonlinear effect in the fiber, the spectrum of which features Kelly sidebands [Fig. 5(b)]. Numerical simulation confirms the existence of pulse

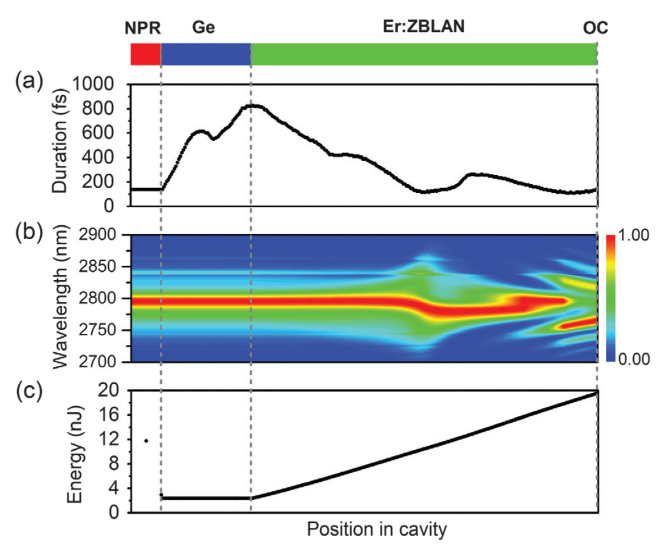

Fig. 5 Numerical simulation of a breathing-pulse MLFFL consisting of an NPR system, a Ge rod, an Er:ZBLAN fiber, and an OC. Evolution of (a) pulse duration, (b) spectrum, and (c) pulse energy along the cavity.

breathing along the cavity with a pulse breathing ratio of 6 [Fig. 5(a)], which significantly reduces the averaged peak power and avoids the excessive accumulation of nonlinear phase shift in the fiber. Consequently, the pulse energy can be linearly scaled up in the fiber without pulse break-up [Fig. 5(c)]. The irregular change of pulse duration in the Ge rod and fiber is attributed to the influence of third-order dispersion in these materials.

Dispersion management is the key to drive MLFFLs from the soliton to the breathing-pulse mechanism. Without dispersion management, the MLFFL generally operates in a soliton mode-locking regime, in which the pulse energy is limited by the soliton area theorem. In our case, the pulse energy is limited to 5.6 nJ in a soliton mode-locking regime. With dispersion management by means of a Ge rod, the MLFFL is no longer confined to a soliton regime. Dispersion-managed MLFFL transforms from soliton to breathing pulse regime, in which the intracavity pulse is stretched and compressed successively owing to the coexistence of normal and anomalous dispersion; the intracavity pulse finally evolves into a soliton pulse since the intracavity net dispersion remains negative. We recognize that the laser is still in the framework of dispersion-managed soliton because it is substantially a dispersion-managed cavity, but the breathing pulse is a new form of dispersion-managed soliton. The pulse-breathing effect significantly reduces nonlinear-phase-shift accumulation and relaxes the pulse-energy limitation in MLFFL. Pulse energy of MLFFL is scaled up to 9.3 nJ with a record peak power of 43.3 kW. Higher peak power is only constrained by damage risk of fluoride fiber end face. Provided that the fluoride fiber is spliced to a protective end cap and intracavity dispersion is further optimized, a higher pulse energy and peak power is expected to be generated from a breathing-pulse MLFFL. Although further increasing the normal dispersion to the net normal dispersion regime in the cavity, the mode-locked pulse evolves to the picosecond regime. For example, using a 20-cm Ge rod to compensate for the anomalous dispersion of a 3.0-m fluoride fiber at a net intracavity dispersion of $+0.087\ \mathrm{ps}^2$, a 1.78-ps pulse is achieved with a spectral bandwidth of 18 nm (see Fig. S1 in the Supplementary Material). In addition to dispersion management inside an oscillator, Ge can also be used as a reliable mid-IR dispersive component to stretch or compress pulses for the chirped pulse amplification with fluoride fibers in the future.

In conclusion, by utilizing the huge normal GVD generated near the absorption edge of Ge for mid-IR dispersion management, we realized breathing-pulse mode-locking, which mitigates the pulse-energy limitation in MLFFLs. The properties of Ge, including its low loss, large normal GVD, and easy installation, make it a reliable and practical dispersion management method for mid-IR rare-earth-doped (Er^{3+}, Ho^{3+}, and Dy^{3+}) fluoride fiber lasers. With intracavity dispersion management, mid-IR MLFFLs are no longer confined to a soliton mode-locking regime. Here we demonstrated breathing-pulse mode-locking in an Er:ZBLAN fiber laser, in which the intracavity pulse is stretched and compressed successively, resulting in reduced nonlinear-phase-shift accumulation and permitting the generation of a high pulse energy. Finally, we achieved a pulse energy of 9.3 nJ and a pulse duration of 215 fs with a record peak power of 43.3 kW from a breathing-pulse mode-locked Er:ZBLAN fiber laser at 2.8 μm. Our work paves the way for the pulse-energy and peak-power scaling of mid-IR MLFFLs, which will enable a wide range of applications, such as supercontinuum generation, material modification, medical surgery, and mid-IR ultrafast spectroscopy.

Acknowledgments

The work was partially supported by the National Natural Science Foundation of China (Grant Nos. 61675130, 91850203, and 11721091) and the National Postdoctoral Program for Innovative Talents (Grant No. BX20170149).

References

1. S. D. Jackson, "Towards high-power mid-infrared emission from a fibre laser," *Nat. Photonics* **6**(7), 423–431 (2012).
2. X. Zhu et al., "Pulsed fluoride fiber lasers at 3 μm," *J. Opt. Soc. Am. B* **34**(3), A15–A28 (2017).
3. G. Ycas et al., "High-coherence mid-infrared dual-comb spectroscopy spanning 2.6 to 5.2 μm," *Nat. Photonics* **12**(4), 202–208 (2018).
4. J. Ma et al., "Review of mid-infrared mode-locked laser sources in the 2.0 μm-3.5 μm spectral region," *Appl. Phys. Rev.* **6**(2), 021317 (2019).
5. C. Zhu et al., "A robust and tuneable mid-infrared optical switch enabled by bulk Dirac fermions," *Nat. Commun.* **8**, 14111 (2017).
6. S. Antipov et al., "High-power mid-infrared femtosecond fiber laser in the water vapor transmission window," *Optica* **3**(12), 1373–1376 (2016).
7. S. Duval et al., "Femtosecond fiber lasers reach the mid-infrared," *Optica* **2**(7), 623–626 (2015).
8. T. Hu, S. D. Jackson, and D. D. Hudson, "Ultrafast pulses from a mid-infrared fiber laser," *Opt. Lett.* **40**(18), 4226–4228 (2015).
9. Y. Wang et al., "Ultrafast Dy^{3+}: fluoride fiber laser beyond 3 μm," *Opt. Lett.* **44**(2), 395–398 (2019).
10. C. R. Petersen et al., "Mid-infrared supercontinuum covering the 1.4-13.3 μm molecular fingerprint region using ultra-high NA chalcogenide step-index fibre," *Nat. Photonics* **8**(11), 830–834 (2014).
11. Y. Tang et al., "Generation of intense 100 fs solitons tunable from 2 to 4.3 μm in fluoride fiber," *Optica* **3**(9), 948–951 (2016).
12. A. H. Nejadmalayeri et al., "Inscription of optical waveguides in crystalline silicon by mid-infrared femtosecond laser pulses," *Opt. Lett.* **30**(9), 964–966 (2005).
13. K. Tamura et al., "77-fs pulse generation from a stretched-pulse mode-locked all-fiber ring laser," *Opt. Lett.* **18**(13), 1080–1082 (1993).
14. Y. Cui and X. Liu, "Graphene and nanotube mode-locked fiber laser emitting dissipative and conventional solitons," *Opt. Express* **21**(16), 18969–18974 (2013).
15. W. H. Renninger, A. Chong, and F. W. Wise, "Dissipative solitons in normal-dispersion fiber lasers," *Phys. Rev. A* **77**(2), 023814 (2008).
16. B. Oktem, C. Ülgüdür, and F. Ömer Ilday, "Soliton-similariton fibre laser," *Nat. Photonics* **4**(5), 307–311 (2010).
17. W. Liu et al., "Femtosecond Mamyshev oscillator with 10-MW-level peak power," *Optica* **6**(2), 194–197 (2019).
18. F. Gan, "Optical properties of fluoride glasses: a review," *J. Non-Cryst. Solids* **184**, 9–20 (1995).
19. N. P. Barnes and M. S. Piltch, "Temperature-dependent Sellmeier coefficients and nonlinear optics average power limit for germanium," *J. Opt. Soc. Am.* **69**(1), 178–180 (1979).
20. X. Meng et al., "Watt-level widely tunable femtosecond mid-infrared $KTiOAsO_4$ optical parametric oscillator pumped by a 1.03 μm Yb:KGW laser," *Opt. Lett.* **43**(4), 943–946 (2018).
21. J. Fan et al., "High power 4.2-cycle mid-infrared pulses from a self-compression optical parametric oscillator," *IEEE Photonics J.* **10**(6), 1504807 (2018).
22. C. Agger et al., "Supercontinuum generation in ZBLAN fibers—detailed comparison between measurement and simulation," *J. Opt. Soc. Am. B* **29**(4), 635–645 (2012).

Zhipeng Qin is an assistant research fellow in the School of Physics and Astronomy, Shanghai Jiao Tong University. He received his PhD in physics from Shanghai Jiao Tong University in 2017. From 2017 to

2019, he was engaged in postdoctoral research at Shanghai Jiao Tong University, and then joined the School of Physics and Astronomy at Shanghai Jiao Tong University. His current research interests include mid-infrared ultrafast fiber lasers and nonlinear optics.

Guoqiang Xie is a professor in the School of Physics and Astronomy, Shanghai Jiao Tong University. He received his PhD from the Department of Optical Science and Engineering, Fudan University in 2008. From 2006 to 2009, he was engaged in research in the School of Electrical and Electronic Engineering, Nanyang Technological University, Singapore. In 2009, he joined the School of Physics and Astronomy, Shanghai Jiao Tong University. He has published over 100 peer-review papers which have been cited over 2300 times. His current research interests include midinfrared ultrashort laser, midinfrared intense laser, vortex laser, and related laser applications.

Liejia Qian received his PhD in optics from Shanghai Institute of Optics and Fine Mechanics (SIOM), Chinese Academy of Sciences in 1989. From 1991 to 1993, he was a postdoctoral researcher at Politecnico de Milano, Italy. In 1993, he joined SIOM as a senior researcher. He spent the academic years of 1997 to 1999 at the Department of Applied Physics, Cornell University. After six years in the chair position at the Department of Optical Science and Engineering, Fudan University, since 2009 he has been a distinguished professor in the Physics Department of Shanghai Jiao Tong University. He has published over 100 papers in internationally indexed journals and owns 25 patents. His research works are in the direction of ultrafast nonlinear optics and intense laser engineering.

Biographies of the other authors are not available.